www.czasopisma.pan.pl PAN www.journals.pan.pl

JOURNAL OF WATER AND LAND DEVELOPMENT
e-ISSN 2083-4535
Polish Academy of Sciences (PAN) Institute of Technology and Life Sciences – National Research Institute (ITP – PIB)

JOURNAL OF WATER AND LAND DEVELOPMENT
DOI: 10.24425/jwld.2021.138161
2021, No. 50 (VI–IX): 64–68

Effect of temperature in removing of anions in solution on biochar using *Zea mays* stalks as a precursor

Ángel Villabona-Ortiz[1], Candelaria Tejada-Tovar[1], Rodrigo Ortega-Toro[2]

[1] Universidad de Cartagena, Faculty of Engineering, Department of Chemical Engineering, Cartagena de Indias, Colombia

[2] Universidad de Cartagena, Faculty of Engineering, Department of Food Engineering, Avenida Del Consulado 48-152, Cartagena 130014, Colombia

RECEIVED 25.08.2020 REVIEWED 20.11.2020 ACCEPTED 27.11.2020

Abstract: Biochar was prepared from corn (*Zea mays*) stalks and impregnated with sulfuric acid. The biomass was impregnated for 24 h with a 50% solution of H_2SO_4 with impregnation ratios 1:2 (B 1:2) and 1:3 p/v (B 1:3); then, it was carbonized in a muffle furnace at 520°C for 30 min with a 10°C per min ramp. The adsorption capacity to remove anions (nitrate, sulfate, and phosphate) in an aqueous solution was evaluated by varying the temperature. The adsorption mechanism was studied by determining the thermodynamic parameters: Gibbs free energy (ΔG^o), enthalpy (ΔH^o) and entropy (ΔS^o) standard. The biochars were characterized by Scanning Electron Microscopy-Energy Dispersive X-Ray Spectroscopy (SEM-EDS) analysis and were found to exhibit a heterogeneous surface and porous nature, with C, O, S, and Si. The experiments in the batch system showed the best performance of B 1: 2 in the removal of the three anions occurred at 303 K, while B 1: 3 had the best performance at 298 K. From the thermodynamic parameters, it was found that the removal processes are endothermic, their mechanism is by chemisorption. It is concluded that synthesized biochar is an excellent alternative to removing nutrient anions present in the solution.

Keywords: adsorption, biochar, cornstalks, nitrate, sulfate, phosphate

INTRODUCTION

The discharge of pollutants rich in nitrogen, sulfur, and phosphorus make higher contributions to the eutrophication of water [Wurtsbaugh *et al.* 2019]; with the entry of these substances into water bodies being the first step in triggering eutrophication in aquatic systems [Stebbins *et al.* 2019]. Thus, eutrophication causes excessive enrichment of surface water with nutrients that promote autotrophic beings' reproduction, mainly algae and cyanobacteria; this causes hypoxia or anoxia in poorly mixed waters [Beusekom van 2017].

The entry of nitrates, sulfates, and phosphates into water bodies and their accumulation is attributed to anthropogenic sources: domestic and industrial wastewater, detergents, animal excrements, and fertilizers [Boeykens *et al.* 2017]. The intake of nitrate in high concentrations causes gastric diseases, congenital disabilities, cardiovascular diseases, thyroid damage, and vaccine cyanosis [Ward *et al.* 2018]. In addition, sulfate anions can lead to increased decomposition of organic matter, increased phosphate mobilization, and dissolved sulfur accumulation [Fernando *et al.* 2018].

Several conventional methods are used to remove water pollutants, such as membrane technologies, solar/UV degradation, filtration, electrochemical treatments and adsorption, among others [Fan, Zhang 2018]. Bioadsorption is a frequently used technique because it allows the selective removal of specific solid components from a liquid phase through the use of biological material [Fomina, Gadd 2014], and its success due to the high availability of the precursors of the adsorbents, their reuse capacity, and the straightforward mechanism of the process [Dai *et al.* 2018].

Adsorbents for the removal of nitrate, phosphate, and sulfate have been developed using orange peel as precursor [Karthikeyan, Meenakshi 2019], grapefruit [Akram *et al.* 2020], peel and potato residues [El-Nahas *et al.* 2019], oil palm bagasse [Shang *et al.* 2018], corn residue [Wang *et al.* 2018], which reported good performance in anion removal after surface modification of the structure. Biochars are useful due to their porous structure, low cost, and environmental compatibility; however, it has shown a low adsorption capacity towards anionic species, making it necessary to modify the surface to improve its adsorption capacity. Thus, the objective of the present study was to evaluate the effect of temperature on the adsorption capacity of nitrate (N), sulfate (S), and phosphate (P), using a porous adsorbent prepared from functionalized corn stalks with different sulfuric acid impregnation ratios. The adsorption mechanism was studied by determining the thermodynamic parameters: Gibbs free energy (ΔG°), enthalpy (ΔH°) and entropy (ΔS°). The prepared biochar was characterized by SEM-EDS analysis to study the morphology and surface chemical composition. The pH zero charge point (pHPZC) was also determined to establish the pH value where the surface charge of the adsorbent is zero.

STUDY METHODS

In the experimental design, the adsorption capacity of phosphate, nitrate, and sulfate ions in mg·g^{-1} was defined as a response variable. As the intervening variables, the pH, stirring rate (rpm), the concentration of the adsorbate (mg·dm^{-3}), and the dose of adsorbent (g). As an independent variable, the temperature in five levels: 298, 303, 308, 313, and 318 K. The synthetic solutions at 100 mg·dm^{-3} were prepared using distilled water and monopotassium phosphate (KH_2PO_4), sodium nitrate ($NaNO_3$), and potassium sulfate (K_2SO_4) of analytical grade, with 95% purity Merck Millipore brand. The biochar was activated with sulphuric acid (H_2SO_4). For determining the final concentration of the pollutants, a Biobase UV/Vis Spectrophotometer BK-UV1900 was used.

Preparation of biochar. Corn stalks were collected as post-harvest waste in Maria la Baja (Bolivar, Colombia). The biomaterial was washed with deionized water, dried at 60°C for 12 h, and reduced in size in an electric mill. 50 g of pretreated corn stalks with a particle size of 1–2 mm were used. The biomass was impregnated for 24 h with a 50% solution of H_2SO_4 with impregnation ratios 1:2 (B 1:2) and 1:3 p/v (B 1:3); then, it was carbonized in a muffle furnace at 520°C for 30 min with a 10°C·min^{-1} ramp. The biochar was washed with abundant distilled water until neutral. Finally, it was dried at 100°C for 8 h and stored in airtight containers until used in the adsorption tests [Manjunath, Kumar 2018]. The biofuels were characterized by analysis: Scanning Electron Microscope (SEM) in conjunction with an Energy Dispersion Spectrometer (EDS) to study the morphology and composition of the bio-adsorbent. The zero pH loading point (pHPZC) was determined to establish the pH value where the vast majority of the adsorbent sites are neutrally charged and therefore, the net charge (external and internal) of the particle is zero due to the reactivity of the substance's surface with the H^+ and OH^- ions [Bakatula *et al.* 2018].

Adsorption tests. Adsorption tests were carried out in a batch system with phosphate, nitrate, and sulfate solutions prepared in synthetic solutions. The pH was adjusted with sodium hydroxide (NaOH) and hydrochloric acid (HCl) 1 M. The phosphate solution was prepared by dissolving 439 mg of dehydrated KH_2PO_4 in 1000 cm^3 of water [ASTM D 515-60]. To the nitrate one, KNO_3 was dried in an oven at 103–105°C for 24 h; it was dissolved 0.7218 g ±0.0005 g in deionized water and diluted up to 1000 cm^3. The sample was preserved with 2 cm^3 of chloroform per dm^3 [ASTM D7781-14]. The sulfate solution was prepared by dissolving 0.1479 g of dehydrated Na_2SO_4 in distilled water diluted to 1000 cm^3 [ASTM D 4130-15]. The tests were carried out in 15 cm^3 vials using an adsorbent dose of 2 g·dm^{-3} at the optimum pH of each biochar, at 200 rpm on an orbital shaker at the set temperature conditions (298, 303, 308, 313 and 318 K). The final concentration of phosphates, nitrates and sulphates was determined by UV/Vis at 880 nm, 543 nm and 420 nm, respectively [ASTM D 515-60; ASTM D 4130-15; ASTM D7781-14].

Removal yield and adsorption capacity were determined according to Equations (1) and (2):

$$RY = \frac{C_i - C_f}{C_i} 100 \tag{1}$$

$$q_t = \frac{(C_i - C_f)V}{m} \tag{2}$$

where: *RY* (%) is the removal efficiency, C_i and C_f are the initial and final concentration of the solution (mg·dm^{-3}), q_y is the adsorption capacity of the biochar (mg·g^{-1}), *V* is the volume of solution and (dm^3), *m* is the mass of adsorbent used (g).

Thermodynamic parameters. Thermodynamic parameters such as Gibbs' free energy (ΔG°), enthalpy change (ΔH°), and entropy change (ΔS°) were determined to learn about the nature of adsorption and its thermodynamic behaviour. This fact was done by the Van't Hoff graphical method, summarized in the following equations [Dobrosz-Gómez *et al.* 2018]:

$$\Delta G^\circ = -RT\ln(K_c) \tag{3}$$

$$\ln K_c = \frac{-\Delta H^\circ}{R\,T} + \frac{\Delta S^\circ}{R} \tag{4}$$

where: *R* is the ideal gas constant and has a value of 8.314 J·mol^{-1}·K^{-1}, *T* is the temperature expressed in Kelvin, K_c is the adsorption equilibrium constant.

RESULTS AND DISCUSSION

CHARACTERISATION OF BIOCHAR

As shown in Figure 1, the bio-adsorbents exhibited a heterogeneous surface and porous nature. The B 1:3 ratio was that of the most porous exposed area, attributed to the higher proportion of H_2SO_4 used during the material's impregnation. The pores are in the macro and mesopore range and allow access to the microporous structure, similar to that reported by [Pap *et al.* 2018]. B 1:2 shows the presence of agglutinated networks and a lower presence of pores. The graphitized structure and the degree of aromaticity are affected by the volatilization of oxygen and hydrogen from the lignocellulosic compounds of low aromaticity and lignin of the corn stalks. This fact caused the remaining carbon to form new aromatic bonds [Peiris *et al.* 2019].

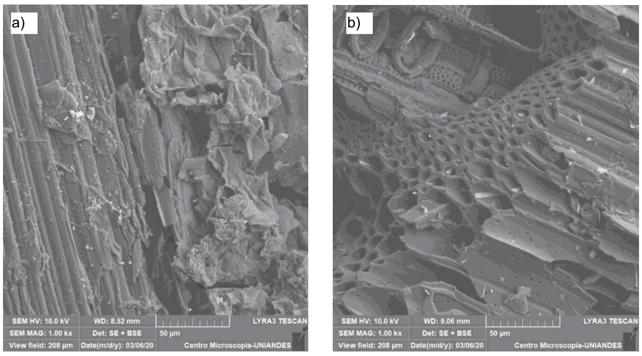

Fig. 1. Scanning electron microscopy for two biochar ratios: a) B 1:2, b) B 1:3; source: own study

From the EDS images, it was observed the presence of C, O, Si, and S atoms, related to the bio-adsorbents; the sulphur related to the impregnation of the biochar with H_2SO_4 evidence the success of the process, considering that the S content of the biochar without impregnation was 2.35% w/w and in the corn stalks 4.3% w/w. A summary of the elemental composition determined by EDS analysis is shown in Table 1.

Figure 2 shows a graph of the final pH versus the initial pH for the differently prepared biochar and calculates the pH_{pzc}. Biochar behaves like a positively charged structure with pH values below pH_{pzc}.

Table 1. Composition of biochar (B)

Element	Percentage by weight (% w/w)	
	B 1:2	B 1:3
C	75.86	72.55
O	11.75	16.74
Mg	–	0.40
Si	1.67	0.79
P	–	0.33
S	10.72	5.48
K	–	2.97
Ca	–	0.74

Source: own study.

After increasing the solution's pH, the bio-adsorbents behave similarly because of the deprotonation of their surface [Hassan *et al.* 2017]. The pH_{pzc} of B 1:2 was 2.95, and B 1:3 was 3.65, indicating that pH values above this value should have a negatively charged surface [Izquierdo 2010]. Different authors have reported similar values for the pH_{pzc} in carbons activated with sulfuric acid using precursors of different biomaterials of lignocellulosic origin: Peiris *et al.* [2019] found a pH_{pzc} of 3.5, while 4.56 was reported by Pap *et al.* [2018] found this property at 4.5. It is observed that the range of the reported values is between 2 and 5. The synthesized biochar has acid groups on its surface due to the impregnation with H_2SO_4 at 50% v/v. The low pH of B 1:2 and B 1:3 can be attributed to increased hydron cations or the decrease of hydroxyl anions [Fan, Zhang 2018]. Considering that the synthesized biofuels will be used to remove anions, it is considered that by using the pHs of the solution below the pH_{pzc}, they would positively charge the material's surface, promoting the adsorption of the solution anionic contaminant. Thus, it was established that the optimum operating pH for B 1: 2 was 2.5, and for B 1: 3, it was 3.5.

EFFECT OF TEMPERATURE

The operational pH for the bio-adsorption process of each anion with the biochar has been defined (2.5 and 3.5 for B 1: 2 and B 1: 3, respectively). The experiments were run at varying temperatures. Figure 3 summarises the results of the effect of temperature on the removal capacity of nitrate (N), sulfate (N), and phosphate (P). The removal best performance of B 1: 2 was at 303 K, while B 1: 3 had the best performance at 298 K. Therefore, it is assumed that the process does not need to be supplied with energy in order for this to happen due to the possible exothermic nature of the reactions. The bio-adsorbents showed selectivity by the phosphate, obtaining the highest adsorption with B 1:2, due to the additional H+ adsorption of the solution on the biochar surface [Zare, Ghasemi-Fasaei 2018].

Table 2 summarises the thermodynamic parameters of nitrate, sulfate, and phosphate adsorption; it is determined that all removal processes present endothermic adsorption due to the negative sign of $\Delta H°$. Thus there is no necessity to supply energy to the system during the process [Bashir *et al.* 2017]. According to its value, chemisorption is suggested for the

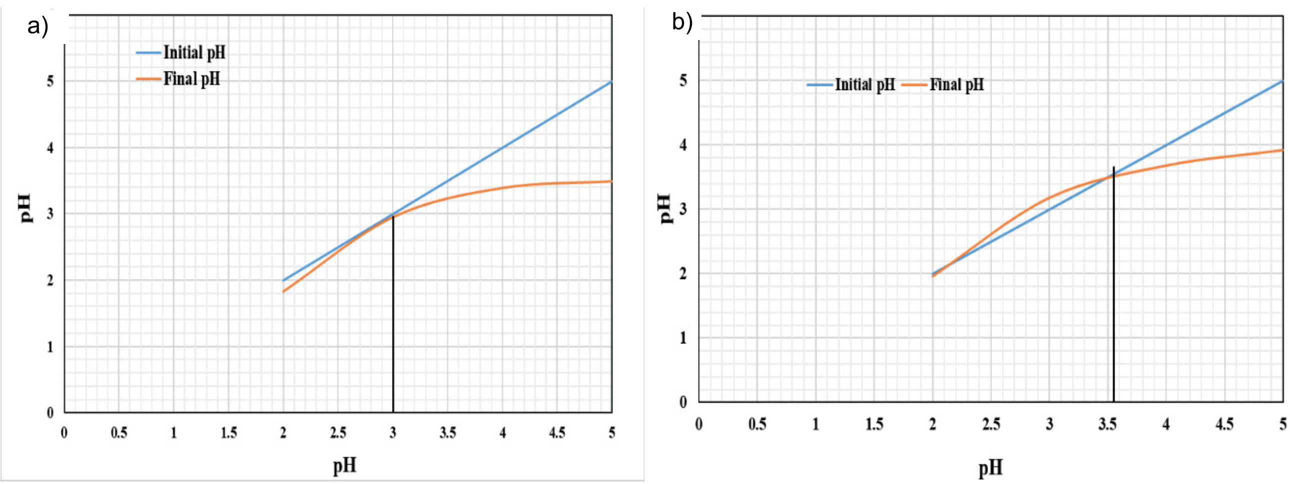

Fig. 2. Zero loading point pH for two biochar ratios: a) B 1:2, b) B 1:3; source: own study

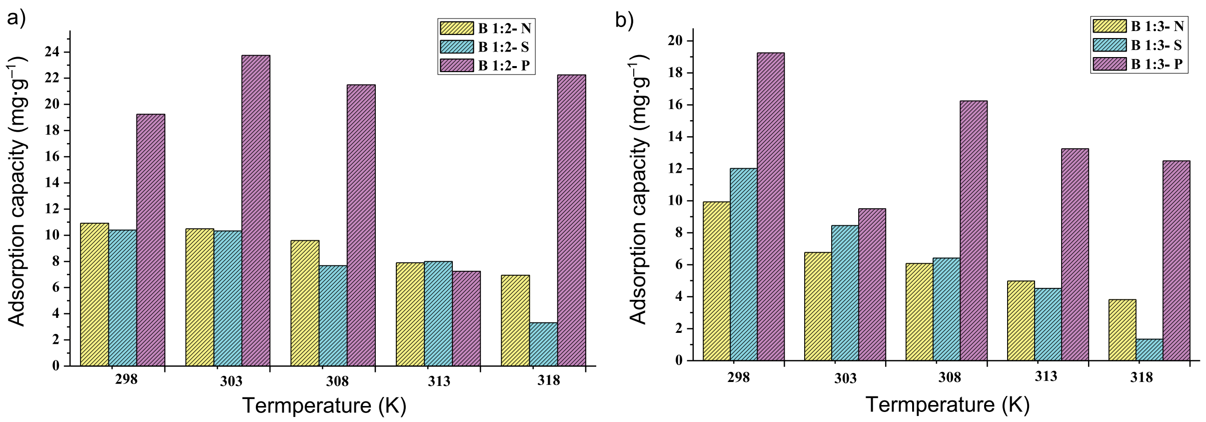

Fig. 3. Effect of temperature on the adsorption capacity of nitrate, sulfate, and phosphate with two biochar ratios: a) B 1:2, b) B 1:3; source: own study

Table 2. Thermodynamic adsorption parameters of nitrate, phosphate and sulfate

Biochar ratio	*T* (K)	Nitrate			Sulfate			Phosphate		
		Δ*G*°	Δ*H*°	Δ*S*°	Δ*G*	Δ*H*°	Δ*S*°	Δ*G*°	Δ*H*°	Δ*S*°
		kJ·mol^{-1}		kJ·mol^{-1} ·K^{-1}	kJ·mol^{-1}		kJ·mol^{-1} ·K^{-1}		kJ·mol^{-1}	kJ·mol^{-1} ·K^{-1}
B 1:2	298	11.619	−22.767	−0.115	10.370	−45.830	−0.189	8.362	−18.850	−0.091
	303	12.197			11.315			8.819		
	308	12.773			12.257			9.275		
	313	13.349			13.199			9.731		
	318	13.926			14.142			10.188		
B 1:3	298	12.248	−40.120	−0.176	9.953	−87.621	−0.327	13.910	−13.302	−0.091
	303	13.126			11.589			14.366		
	308	14.004			13.225			14.823		
	313	14.882			14.862			15.279		
	318	15.760			16.498			15.735		

Source: own study.

processes [Sereshti *et al.* 2020]. The positive values of Δ*G*° indicate that the system is not spontaneous for removing anions using the synthesized biochars. Furthermore, the Δ*G*° increases as the system's temperature increases, the process energetically becomes more favourable [Mehdinejadiani *et al.* 2019]. The negative value of Δ*S*° indicates the removal irreversibility and a low probability of structural changes due to the formation of the bonds between the active centres of the bio-adsorbent and the pollutants [Yin *et al.* 2019].

CONCLUSIONS

1. B 1:3 has a porous structure with macro and mesopores, and B 1:2 show the presence of agglutinated with the presence of pores.

2. The best performance of B 1: 2 in the removal of the three anions was at 303, while B 1: 3 had the best performance at 298 K.

3. Thermodynamic parameters established that the removal processes of the three anions are endothermic. Their mechanism is by chemisorption, the adsorption is favourable with a probability of structural changes by the formation of the bonds between the active centres of the bio-adsorbent and the pollutants. From the results, it is determined that biochar is a good alternative for removing nutrient anions present in the solution.

ACKNOWLEDGEMENTS

The authors would like to acknowledge the Universidad de Cartagena for providing the materials, equipment, and research time required to conclude this research successfully.

REFERENCES

Akram M., Xing X., Baoyu G., Qinyan Y., Shang Y., Rizwan K., Inam M.A. 2020. Adsorptive removal of phosphate by the bimetallic hydroxide nanocomposites embedded in pomegranate peel. Journal of Environmental Sciences. Vol. 91 p. 189–198. DOI 10.1016/j.jes.2020.02.005.

ASTM D 515-60 T tentative methods of test for phosphate in industrial water. In: Manual on industrial water and industrial waste water. West Conshohocken, PA. American Society for Testing and Materials p. 237–245. DOI 10.1520/STP48521S.

ASTM D4130-15 Standard test method for sulfate in brackish water, seawater, and brines. West Conshohocken, PA. American Society for Testing and Materials pp. 5. DOI 10.1520/D4130-15.

ASTM D7781-14 Standard test method for nitrite-nitrate in water by nitrate reductase. West Conshohocken, PA. American Society for Testing and Materials pp. 7. DOI 10.1520/D7781-14.

Bakatula E.N., Richard D., Neculita C.M., Zagury G.J. 2018. Determination of point of zero charge of natural organic materials. Environmental Science and Pollution Research. Vol. 25 p. 7823–7833. DOI 10.1007/s11356-017-1115-7.

Bashir M.T., Ali S., Idris A., Harun R. 2017. Kinetic and thermodynamic study of nitrate adsorption from aqueous solution by lignocellulose-based anion resins. Desalination and Water Treatment. Vol. 62 p. 449–456. DOI 10.5004/dwt.2017.20136.

Beusekom J.E.E. van. 2017. Eutrophication. Chapt. 22. In: Handbook on marine environment protection. Science, impacts and sustainable management. Eds. M. Salomon, T. Markus. Springer Intern. Publ. p. 429–445. DOI 10.1007/978-3-319-60156-4_22.

Boeykens S.P., Piol M.N., Samudio Legal L., Saralegui A.B., Vázquez C. 2017. Eutrophication decrease: Phosphate adsorption processes in presence of nitrates. Journal of Environmental Management Vol. 203 p. 888–895. DOI 10.1016/j.jenvman.2017.05.026.

Dai Y., Sun Q., Wang W., Lu L., Liu M., Li J., ..., Zhang Y. 2018. Utilizations of agricultural waste as adsorbent for the removal of contaminants: A review. Chemosphere. Vol. 211 p. 235–253. DOI 10.1016/j.chemosphere.2018.06.179.

Dobrosz-Gómez I., Gómez M., Santa C. 2018. Optimización del proceso de adsorción de Cr(VI) sobre carbón activado de origen bituminoso [Optimization of the Cr(VI) adsorption process on bituminous activated carbon]. Información Tecnológica. Vol. 29. No. 6 p. 43–56. DOI 10.4067/S0718-07642018000600043.

El-Nahas S., Salman H.M., Seleeme W.A. 2019. Aluminum building scrap wire, take-out food container, potato peels and bagasse as valueless waste materials for nitrate removal from water supplies. Chemistry Africa. Vol. 2 No. 1 p. 143–162. DOI 10.1007/s42250-018-00032-z.

Fan C., Zhang Y. 2018. Adsorption isotherms, kinetics and thermodynamics of nitrate and phosphate in binary systems on a novel adsorbent derived from corn stalks. Journal of Geochemical Exploration. Vol. 188 p. 95–100. DOI 10.1016/j.gexplo.2018.01.020.

Fernando W..A.M., Ilankoon I.M.S.K., Syed T.H., Yellishetty M. 2018. Challenges and opportunities in the removal of sulphate ions in contaminated mine water: A review. Minerals Engineering. Vol. 117 p. 74–90. DOI 10.1016/j.mineng.2017.12.004.

Fomina M., Gadd G.M. 2014. Biosorption: current perspectives on concept, definition and application. Bioresource Technology Vol. 160 p. 3–14. DOI 10.1016/j.biortech.2013.12.102.

Hassan W., Farooq U., Ahmad M., Athar M., Khan M. 2017. Potential biosorbent, haloxylon recurvum plant stems, for the removal of methylene blue dye. Arabian Journal of Chemistry Vol. 10 p. 1512–1522. DOI 10.1016/j.arabjc.2013.05.002.

Izquierdo M. 2010. Eliminacion de metales pesados en aguas mediante bioadsorcion. Evaluacion de materiales y modelacion del proceso [Elimination of heavy metals in water by bioadsorption. Materials evaluation and process modeling] [online]. PhD Thesis. Universitat de València. ISBN 9788437079813 pp. 352. [Access 20.07.2020]. Available at: http://hdl.handle.net/10803/52130.

Karthikeyan P., Meenakshi S. 2019. Synthesis and characterization of Zn–Al LDHs/activated carbon composite and its adsorption properties for phosphate and nitrate ions in aqueous medium. Journal of Molecular Liquids Vol. 296, 111766. DOI 10.1016/j.molliq.2019.111766.

Manjunath S. V., Kumar M. 2018. Evaluation of single-component and multi-component adsorption of metronidazole, phosphate and nitrate on activated carbon from prosopıs julıflora. Chemical Engineering Journal. Vol. 346 p. 525–534. DOI 10.1016/j.cej.2018.04.013.

Mehdinejadiani B., Amininasab S.M., Manhooei L. 2019. Enhanced adsorption of nitrate from water by modified wheat straw: Equilibrium, kinetic and thermodynamic studies. Water Science and Technology. Vol. 79. No. 2 p. 302–313. DOI 10.2166/wst.2019.047.

Pap S., Bezanovic V., Radonic J., Babic A., Saric S., Adamovic D., Turk Sekulic M. 2018. Synthesis of highly-efficient functionalized biochars from fruit industry waste biomass for the removal of chromium and lead. Journal of Molecular Liquids. Vol. 268 p. 315–325. DOI 10.1016/j.molliq.2018.07.072.

Peiris C., Nayanathara O., Navarathna C.M., Jayawardhana Y., Nawalage S., Burk G., …, Gunatilake S.R. 2019. The influence of three acid modifications on the physicochemical characteristics of tea-waste biochar pyrolyzed at different temperatures: A comparative study. RSC Advances. Vol. 9. No. 31 p. 17612–17622. DOI 10.1039/c9ra02729g.

Sereshti H., Zamiri Afsharian E., Esmaeili Bidhendi M., Rashidi Nodeh H., Afzal Kamboh M., Yilmaz M. 2020. Removal of phosphate and nitrate ions aqueous using strontium magnetic graphene oxide nanocomposite: Isotherms, kinetics, and thermodynamics studies. Environmental Progress and Sustainable Energy. Vol. 39. No. 2, e13332 pp. 12. DOI 10.1002/ep.13332.

Shang Y., Guo K., Jiang P., Xu X., Gao B. 2018. Adsorption of phosphate by the cellulose-based biomaterial and its sustained release of laden phosphate in aqueous solution and soil. International Journal of Biological Macromolecules. Vol. 109 p. 524–534. DOI 10.1016/j.ijbiomac.2017.12.118.

Stebbins A., Algeo T.J., Krystyn L., Rowe H., Brookfield M., Williams J., Nye S.W., Hannigan R. 2019. Marine sulfur cycle evidence for upwelling and eutrophic stresses during early Triassic cooling events. Earth-Science Reviews. Vol. 195 p. 68–82. DOI 10.1016/j.earscirev.2018.09.007.

Wang L., Xu Z., Fu Y., Chen Y., Pan Z., Wang R., Tan Z. 2018. Comparative analysis on adsorption properties and mechanisms of nitrate and phosphate by modified corn stalks. RSC Advances. Vol. 8. No. 64 p. 36468–36476. DOI 10.1039/C8RA06617E.

Ward M.H., Jones R.R., Brender J.D., de Kok T.M., Weyer P.J., Nolan B.T., Villanueva C.M., van Breda S.G. 2018. Drinking water nitrate and human health: An updated review. International Journal of Environmental Research and Public Health. Vol. 15. No. 7, 1557. DOI 10.3390/ijerph15071557.

Wurtsbaugh W.A., Paerl H.W., Dodds W.K. 2019. Nutrients, eutrophication and harmful algal blooms along the freshwater to marine continuum. WIREs: Water. Vol. 238 p. 599–606. DOI 10.1002/wat2.1373.

Yin Q., Liu M., Ren H. 2019. Biochar produced from the co-pyrolysis of sewage sludge and walnut shell for ammonium and phosphate adsorption from water. Journal of Environmental Management. Vol. 249, 109410. DOI 10.1016/j.jenvman.2019.109410.

Zare L., Ghasemi-Fasaei R. 2018. Investigation of equilibrium isotherm and kinetic modeling to asses sorption characteristics of nitrate onto palm leaf biochar. Iranian Journal of Chemistry and Chemical Engineering (IJCCE). Vol. 38. No. 5 p. 143–153. DOI 10.30492/IJCCE.2019.31987.